Journal of Organometallic Chemistry 694 (2009) 2163–2170

Contents lists available at ScienceDirect

Journal of Organometallic Chemistry

journal homepage: www.elsevier.com/locate/jorganchem

# Dioxime and pyridine-2-aldoxime complexes of $Re(CO)_3^+$

Roshinee Costa [a], Natalie Barone [a], Christopher Gorczycka [b], Ernest F. Powers [b], William Cupelo [b], Joseph Lopez [b], Richard S. Herrick [b], Christopher J. Ziegler [a,*]

[a] Department of Chemistry, University of Akron, Akron, OH 44325-3601, USA
[b] Department of Chemistry, College of the Holy Cross, Worcester, MA 01610, USA

ARTICLE INFO

*Article history:*
Received 10 December 2008
Received in revised form 19 February 2009
Accepted 20 February 2009
Available online 5 March 2009

*Keywords:*
Rhenium carbonyl
Dioxime
Pyridine-2-aldoxime

ABSTRACT

We present the synthesis and characterization of a series of dioxime and pyridine-2-aldoxime complexes of rhenium(I) tricarbonyl. Complexes of the formula $ReL(CO)_3X$ (L = dioxime (**1**,**2**), dimethylglyoxime (**3**,**4**), diphenylglyoxime (**5**,**6**), 1,2-cyclohexanedione dioxime (**7**,**8**); X = Cl, Br) can be readily generated by reaction of the neutral ligand with $Re(CO)_5X$ (X = Cl, Br) or $[Re(CO)_3(H_2O)_3]Br$. A similar set of pyridine-2-aldoximes of the formula $ReL(CO)_3X$ (L = pyridine-2-aldoxime (**9**,**10**), 2-pyridylamidoxime (**11**,**12**); X = Cl, Br) can also be synthesized in an analogous fashion. Compounds **1**–**6**, **9** and **12** were characterized by single crystal X-ray diffraction. These complexes all exhibit bidentate coordination of the oxime ligands as well as the expected facial arrangement of carbonyls around the metals with the halides completing the octahedral coordination spheres. The oxime groups remain protonated in all of the complexes. Compounds **1–12** all exhibit absorptions in the UV–Vis region resulting from MLCT transitions.



## 1. Introduction

Because of their stability as well as their interesting chemical, physical, and biological properties, there have been numerous studies of organometallic and coordination compounds with α-diimines. Examples of complexes of diimines can be found across the transition metals [1], and $d^6$ complexes, such as those of group 7, have been much studied [2]. The types of diimines that have been investigated can be broken down into ligands with two, one, or no basic heterocycles as part of the α-diimine (Scheme 1), as shown for the 2,2'-bipyridine ligand [1a], pyridinecarbaldehyde imine (pyca) ligand [2d] and diazabutadiene (dab) [3], respectively. The pyca and dab ligands have been prepared with a variety of aliphatic and aromatic amines [4] including amino acids, amino esters and amino alcohols [5].

Less has been reported of group 7 $d^6$ compounds with pyca or dab ligands that have heteroatoms attached to the imine nitrogen(s) (Scheme 1) [6]. There have been several studies by Abram and coworkers that report several thiosemicarbazone complexes of rhenium(I) [6c,6d,6e,6f,6g,6j]. Surprisingly, the very common dioxime family of ligands has not been extensively studied with this family of transition metal ions. Notably, this includes the common dimethylglyoxime (DMG) ligand. Recently, we have been investigating the fundamental chemistry of the $Re(CO)_3^+$ fragment, in large part motivated by the use of this unit as a model for $Tc(CO)_3^+$ based imaging agents as well as $^{186/188}Re$ radionuclide therapeutics. We are interested in exploring unstudied ligands and, in light of this overall goal, we have presented reports on both monodentate and tridentate ligand systems over the past several years [7]. We have turned to DMG and related ligands to create a series of $Re(CO)_3$(bidentate-oxime)X compounds where X = Cl and Br. The DMG chelate and related ligands are intriguing because of their relevance to the clathrochelate, $^{99m}Tc$(III) BATOS complex [8] which has been used for the labeling of antibodies [9]. In addition, the analogous pyridine-2-aldoxime complexes of $d^6$ complexes have also not been explored, in spite of the ready availability of compounds, such as pyridine-2-aldoxime and 2-pyridylamidoxime.

This paper reports the fundamental chemistry of $ReL(CO)_3X$ complexes where L is either a dioxime or a pyridine-2-aldoxime and X is either chloride or bromide (Scheme 2). Complexes of the formula $ReL(CO)_3X$ (L = dioxime (DHG **1**,**2**), dimethylglyoxime (DMG **3**,**4**), diphenylglyoxime (DPG **5**,**6**), cyclohexane dione dioxime (CHDD **7**,**8**); X = Cl, Br) can be readily generated by reaction of the neutral ligand with $Re(CO)_5X$ (X = Cl, Br) or solutions containing $[Re(CO)_3(H_2O_3)]Br$. A similar set of pyridine-2-aldoximes of the formula $Re(L)(CO)_3X$ (L = pyridine-2-aldoxime (**9**,**10**), 2-pyridylamidoxime (**11**,**12**); X = Cl, Br) can also be synthesized in an analogous fashion. Nearly all of the complexes can be generated in high yield; the bromide derivatives can also be prepared using the $Re(CO)_3(H_2O)_3^+$ cation. The resulting compounds exhibit dynamic behavior, as shown by $^1H$ NMR spectroscopy, as well as charge transfer transitions in the visible region. We believe that these compounds might prove useful as targets for bifunctional

* Corresponding author.
*E-mail addresses:* rherrick@holycross.edu (R.S. Herrick), ziegler@uakron.edu (C.J. Ziegler).

0022-328X/$ - see front matter © 2009 Elsevier B.V. All rights reserved.
doi:10.1016/j.jorganchem.2009.02.024

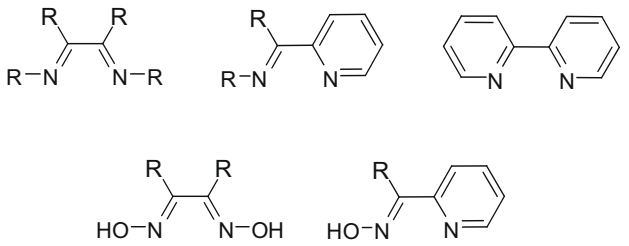

**Scheme 1.** Representative α-diimine ligands including dioxime (bottom left) and pyridine-2-oxime (right).

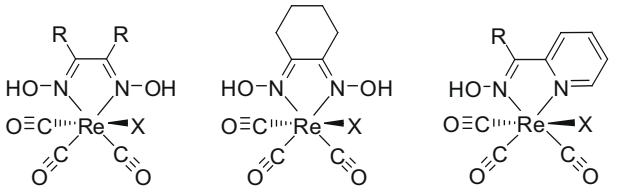

1: R = H, X = Cl
2: R = H, X = Br
3: R = Me, X = Cl
4: R = Me, X = Br
5: R = Ph, X = Cl
6: R = Ph, X = Br

7: X = Cl
8: X = Br

9: R = H, X = Cl
10: R = H, X = Br
11: R = $NH_2$, X = Cl
12: R = $NH_2$, X = Br

**Scheme 2.**

chelating agent (BFCA) design [5d]. By replacement of the halides, a targeting moiety could be attached to the Re tricarbonyl dioxime fragment via attachment of a monodentate ligand, such as a isonitrile, pyridine or imidazole [10].

## 2. Results and discussion

### 2.1. Synthesis

In spite of the prevalent nature of oxime ligands in transition metal chemistry, only six examples of N-bound rhenium oximes have been deposited with the CCDC database [11]. Of these six complexes, the majority are higher valent states (+3,+5) of rhenium, and only one incorporates the $Re(CO)_3$ moiety. Several structures are Re(III) analogs of the $^{99m}$Tc(III) BATOS clathrochelate complex. The single Re(I) example is composed of a bidentate 1,10-phenanthroline and a monodentate acetone N-oxime to $Re(CO)_3^+$. The oxime binds to the metal through the nitrogen and in the neutral form, with charge balance being provided for the Re(I) cation by a non-coordinating tetrakis(3,5-bis(trifluoromethyl)phenyl)borate. The Re–N bond is 2.18 Å, and the C–N bond of the oxime measures 1.26 Å. The complex deviates slightly from an ideal octahedral geometry; the bidentate phenanthroline has an N–Re–N bond angle of ~ 76°, and the oxime is tilted slightly toward the phenantholine, with $N_{oxime}$—Re—$N_{phen}$ bonds of 83° and 86°. The N-bound oxime can be converted to an O-bound oxime on either reaction of the precursor $Re(phen)(CO)_3(OTf)$ with deprotonated oxime or upon reaction of the N-bound oxime with a base [11e]. The O-bound oximato ligand is labile, and can be readily replaced with a series of unsaturated electrophiles.

The $Re(CO)_3X$ complexes of DHG, DMG, DPG and CHDD, where X = Cl and Br (compounds **1**-**8**, respectively) can be readily synthesized by reaction of $Re(CO)_5X$ or $[Re(CO)_3(H_2O_3)]Br$ with a stoichiometric amount of ligand. The solvent system for reactions of DHG, DMG and DPG with $Re(CO)_5X$ is methanol. For the CHDD ligand, methanol did not provide the desired product so benzene was used instead. The reactions were carried out at reflux typically for 4–5 h, however, the CHDD reactions required 24 h for completion. Alternatively, reactions of the ligands with $[Re(CO)_3(H_2O_3)]Br$ in water required only 30 min. Maximum yields were obtained by adding the reagents to the flask prior to the addition of solvent. As the reactions proceeded, the solutions turned from colorless to orange or brown. Typically, pure product in high yield could be obtained by simple evaporation of the solvent and washing of the resultant solid, however, for the CHDD reactions, column chromatography using silica with 15% methanol in ethyl acetate was required to isolate the pure complexes. All of the reactions afforded pure crystalline solids; the DHG, DMG, and DPG complexes are all orange, while the CHDD complexes have a yellow-brown hue. The $Re(CO)_3X$ complexes of pyridine-2-aldoxime and 2-pyridylamidoxime, where X = Cl and Br (compounds **9–12**), were generated in an identical fashion as the dioxime complexes described above using methanol as the solvent. The reaction solutions also changed color as the reaction proceeded to form the colors described above. High purity material of **9–12** can be produced without chromatography via recrystallization.

### 2.2. X-ray structure elucidation

The structures of compounds **1–6** were elucidated by single crystal X-ray diffraction (Fig. 1 and Table 1). The structures of $Re(CHDD)(CO)_3X$ (**7** and **8**) were not successfully elucidated due to twinning problems, but connectivity structures from partially solved data sets confirmed the same coordination mode as in the other dioxime complexes. Table 2 lists some of the key bond lengths and angles in these complexes. All of the complexes have slightly distorted octahedral geometries, with the three carbonyls arranged in a facial configuration as expected for $d^6$ $Re(CO)_3^+$ compounds. The dioxime ligands bind to the metal in a bidentate fashion through the nitrogen atoms, and the oxime oxygen atoms remain protonated. The last sites in the coordination spheres of **1–8** are occupied by chloride for **1**, **3**, **5** and **7** and bromide for **2**, **4**, **6** and **8**. The C–O bonds of the carbonyls are typical for $Re(CO)_3^+$ complexes with the bond lengths in the range of ~1.14–1.16 Å [7]. The Re–C bonds have standard lengths, with ranges of ~1.87–1.95 Å, and the Re–X bonds are as expected for these complexes. The metal–nitrogen bonds of the dioxime have bond lengths that range between ~2.13 and ~2.16 Å. In diimine complexes of the $Re(CO)_3^+$ fragment, the corresponding Re–N bonds are slightly longer, ranging from ~2.14 to ~2.26 Å [10]. The C=N bonds of the in the DMG complexes average ~1.29 and ~1.31 Å for the chloride and the bromide, respectively. These lengths are comparable to other $d^6$ metal ion dioxime complexes, such as $Tc(DMG)_3Cl$ where the distance is ~1.30 Å, but are longer than those observed in neutral DMG, where the C=N bond is ~1.28 Å [8a]. Such lengthening, which can also be deduced from the MLCT transitions present in these compounds (*vide infra*), is indicative of π back bonding to the metal. In the diimine complexes of $Re(CO)_3^+$, the imine bond lengths exhibit a larger variance, ranging from 1.26 to 1.35 Å [12].

The deformations from an ideal octahedral geometry are small for complexes **1–6**, but they are consistent across the series. The bite angle of the dioxime is significantly less than 90°, averaging approximately 72° for the N–Re–N bond. In addition, the halides are slightly tilted toward the dioxime unit in all six structures. These angles range from 88.99(18)° for the Br–Re–N angle in **4** to a Br–Re–N bond angle of 82.74(15)° for compound **2**. Although there may be a small degree of interaction between the conjugated π system of the dioxime and the halogen, these angles are small overall and may result only from crystal packing forces.

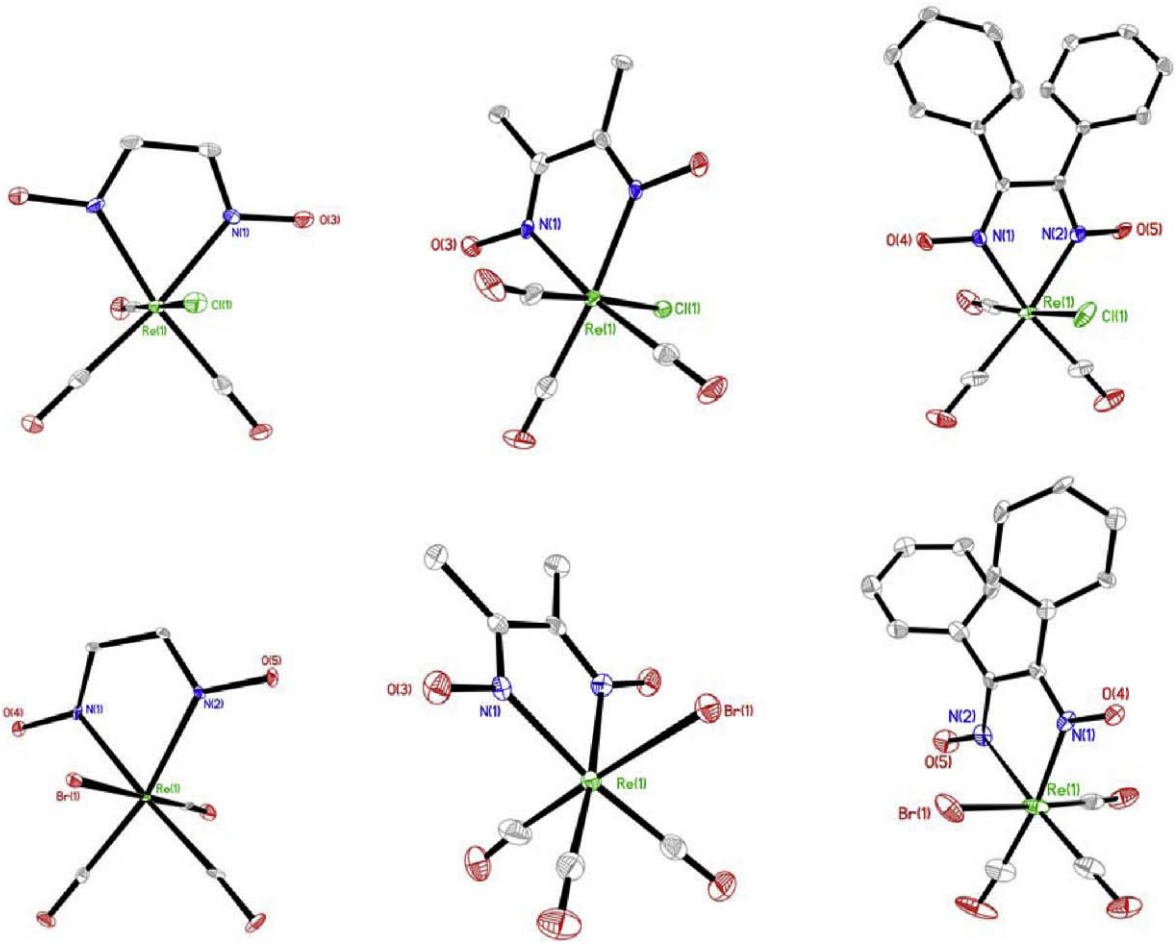


**Fig. 1.** The structures of compounds **1**–**6** with 50% thermal ellipsoids. Hydrogen atoms and solvent molecules have been omitted for clarity.

Two of the four pyridine-2-aldoxime complexes were successfully elucidated by single crystal methods. The structures of compounds **9** and **12** are shown in Fig. 2 and selected bond distances and angles are listed in Table 2. The two complexes are isostructural and closely resemble the dioxime complexes; they both exhibit octahedral geometries with a facial configuration of the carbonyls. The C–O bond lengths average 1.15 Å for both compounds. The Re–C bonds in **9** and **12**, average 1.91 Å. Both metal–halide bond lengths are in the typical range for these $Re(CO)_3X$ complexes. The ligands bind to the metal in a bidentate fashion directly analogous to the dioxime complexes, and the oxime oxygen similarly remains protonated upon coordination. The Re–N bond lengths are longer for the pyridyl nitrogen (2.182(6) for **9** and 2.189(7) for **12**) than for the oxime nitrogen (2.154(6) for **9** and 2.163(7) for **12**), which reflects the difference in basicity between the two ligand types. The disparity in the average pyridyl C=N distances and oxime C=N distances of ~1.36 and ~1.29 Å, respectively, is indicative of the presence of the aromatic ring. These distances are similar to those observed for $Re(CO)_3$(dab-XXX-OR) compounds that we presented in an earlier publication [5e]. As in **1**–**6**, the pyridine-2-aldoxime complexes deviate from ideal octahedral geometries in their N–Re–N bite angle and in the halide tilt. The N–Re–N bonds are in the same range as the dioxime complexes, but compounds **9** and **12** have a slightly larger angles (74.0(2)° and 72.9(3)°). The halide tilts are also oriented toward the bidentate ligand, and range from 81.97(15)° for complex **9** to 86.24(19)° for complex **12**.

### 2.3. Spectroscopic characterization

All of the compounds exhibit carbonyl stretching modes in the IR spectrum that correspond to the pseudo-$C_{3v}$ symmetry ($a_1$ and $e$ modes) of the facial arrangement of the CO units. Due to the reduction from $C_{3v}$ to either $C_s$ or $C_1$ symmetries, the normally degenerate $e$ stretch (lower frequency) splits into two bands. The dioxime complexes **1–8** have $C_s$ symmetries (ignoring the possible conformations of the ligand in the diphenyl complex) while the pyridine-2-aldoxime compounds have $C_1$ symmetries. The splittings are small, on the order of 20–30 $cm^{-1}$. The pyridine-2-aldoxime complexes **9–12** show a larger splitting of the normally degenerate $e$ stretch due to their decreased symmetry, in the range of 30–50 $cm^{-1}$.

The majority of the observed $^1H$ and $^{13}C$ NMR resonances are as expected for these compounds. However, for the DMG and DHG complexes, we observed two sets of resonances for the hydrogens on the dioxime ligand. Similar extra resonances can also be observed in several of the $^{13}C$ NMR spectra. We surmised that the appearance of multiple resonances might result from the conformation of the oxime O–H bond with the hydrogen in this bond toward the carbonyls or facing the hydrogens on the dioxime ligand. In order to investigate this possibility, we collected a $^1H$ NOESY spectrum on **2**. Although the $^1H$ NOESY spectrum seemed to suggest two possible rotational isomers, a follow up variable temperature $^1H$ NMR (VTNMR) spectrum indicated that **2** was actually reacting with solvent rather than engaging in a dynamic process. Fig. 3 shows the effect of increasing heat on a $d^6$-DMSO solution

**Table 1**
X-ray data and structural parameters for compounds **1**–**6**, **9** and **12**.

| | 1 | 2 | 3 | 4 | 5 | 6 | 9 | 12 |
|---|---|---|---|---|---|---|---|---|
| Formula | $ReC_5H_4N_2O_5Cl \cdot 2H_2O$ | $ReC_5H_4N_2O_5Br$ | $ReC_7H_8N_2O_5Cl$ | $ReC_7H_8N_2O_5Br$ | $ReC_{17}H_{12}N_2O_5Cl \cdot 3/16CH_2Cl_2$ | $ReC_{17}H_{12}N_2O_5Br \cdot 1/8CH_3OH$ | $ReC_9H_6N_2O_4Cl \cdot C_4H_8O$ | $ReC_9H_7N_3O_4Br \cdot 1/2CH_3OH$ |
| Formula weight | 429.79 | 438.21 | 421.80 | 466.26 | 561.86 | 594.40 | 499.91 | 503.29 |
| Crystal system | Orthorhombic | Orthorhombic | Orthorhombic | Orthorhombic | Tetragonal | Tetragonal | Monoclinic | Triclinic |
| Space group | *Pnma* | *Pna2(1)* | *Cmca* | *Cmca* | *I4(1)/a* | *I4(1)/a* | *P2(1)/c* | $P\bar{1}$ |
| *a* (Å) | 9.939(9) | 16.385(6) | 10.1309(11) | 10.389(2) | 24.976(4) | 25.516(5) | 14.632(5) | 6.925(3) |
| *b* (Å) | 11.517(11) | 5.856(2) | 18.177(2) | 17.994(2) | 24.976(4) | 25.516(5) | 8.738(3) | 9.657(5) |
| *c* (Å) | 9.682(9) | 9.750(3) | 12.0505(14) | 12.174(2) | 12.464(4) | 12.189(5) | 12.509(5) | 9.966(5) |
| $\alpha$ (°) | 90 | 90 | 90 | 90 | 90 | 90 | 90 | 97.755(8) |
| $\beta$ (°) | 90 | 90 | 90 | 90 | 90 | 90 | 104.306(7) | 97.815(8) |
| $\gamma$ (°) | 90 | 90 | 90 | 90 | 90 | 90 | 90 | 95.473(8) |
| *V* (Å) | 1108.4(18) | 935.6(6) | 2219.1(4) | 2275.7(7) | 7775(3) | 7935(4) | 1549.7(10) | 649.9(6) |
| *Z* | 4 | 4 | 8 | 8 | 16 | 16 | 4 | 2 |
| $\rho$(calc) (Mg/m$^3$) | 2.576 | 3.111 | 2.525 | 2.722 | 1.920 | 1.990 | 2.143 | 2.570 |
| $\mu$ (mm$^{-1}$) | 11.226 | 17.257 | 11.199 | 14.198 | 6.470 | 8.168 | 8.037 | 12.440 |
| *F*(000) | 800 | 792 | 1568 | 1712 | 4286 | 4484 | 952 | 465 |
| Reflections collected | 8593 | 7114 | 9153 | 9264 | 31844 | 15865 | 12588 | 5361 |
| Independent reflections | 1272 | 2033 | 1419 | 1443 | 4230 | 4327 | 3368 | 2783 |
| GOF on $F^2$ | 1.057 | 1.108 | 1.526 | 1.249 | 1.071 | 1.212 | 1.019 | 1.011 |
| $R[I > 2\sigma(I)]$ | $R_1$ = 0.0397, $wR_2$ = 0.0908 | $R_1$ =0.0236, $wR_2$ = 0.0544 | $R_1$ = 0.0473, $wR_2$ = 0.1132 | $R_1$ = 0.0448, $wR_2$ = 0.0953 | $R_1$ = 0.0348, $wR_2$ = 0.0767 | $R_1$ = 0.0845, $wR_2$ = 0.1679 | $R_1$ = 0.0404, $wR_2$ = 0.0821 | $R_1$ = 0.0446, $wR_2$ = 0.0994 |
| *R*(all data) | $R_1$ = 0.0496, $wR_2$ = 0.0946 | $R_1$ = 0.0243, $wR_2$ = 0.0546 | $R_1$ = 0.0492, $wR_2$ = 0.1139 | $R_1$ = 0.0509, $wR_2$ = 0.0973 | $R_1$ = 0.0436, $wR_2$ = 0.0799 | $R_1$ = 0.1163, $wR_2$ = 0.1679 | $R_1$ = 0.0553, $wR_2$ = 0.0862 | $R_1$ = 0.0509, $wR_2$ = 0.1016 |

of **2**. At 40 °C, the spectrum exhibits two peaks for the sp$^2$ hydrogen, 8.20 ppm (98%) and 7.73 ppm (2%). As temperature increases, the 7.73 ppm peak increases and splits at 60 °C into several resonances, and the 8.20 ppm peak decreases and splits as well. With increasing temperature, two products then appear to form in the spectrum, and this spectrum remains unchanged upon cooling. We propose that the complex is reacting with solvent to form a complex such as $[Re(DHG)(CO)_3(DMSO)]^+$. Dimethylsulfoxide complexes of $Re(CO)_3$ are well known [13], and this solvent can bind to the metal in multiple modes, which may account for the multiplicity of peaks. We are continuing our investigations into these reactions as means to generate BFCA complexes with dioxime rhenium complexes.

All twelve complexes are either orange or brown, and each has an absorption band centered in the UV region with a tail extending into the visible region, resulting in the observed hues. Fig. 4 shows the spectra for several of the compounds presented in this report. The energies of these absorptions in methanol range from 351 nm for compound **11** to 392 nm for compound **6**. In all cases, the wavelength of the absorption is greater for the bromide than the chloride complex. We can characterize these absorptions as primarily caused by metal to ligand charge transfer (MLCT) transitions due to the readily observable solvatochromism. As one decreases the polarity of the solvent, such as from methanol to toluene, the MLCT transition undergoes a bathochromic shift. For example, the absorption band in compound **2** appears at 390 nm and 420 nm in methanol and toluene, respectively. The extinction coefficients for these transitions are on the order of ~2000 to 4500 cm$^{-1}$ M$^{-1}$. These values are on the same order of magnitude as those seen in $Re(I)(bpy)(CO)_3L$ complexes [14].

### 2.4. Conclusions

Dioxime and pyridine-2-aldoxime complexes of $Re(CO)_3^+$ can be readily generated by reaction of the ligands with $Re(CO)_5X$ or $[Re(CO)_3(H_2O_3)Br$. These compounds represent a significant addition to the oxime coordination chemistry of d$^6$ metal complexes. In all cases, the resultant complexes are typical Re(I) compounds with a facial arrangement of the carbonyls. The ligands bind in their neutral form, since the oxime ligands remain protonated. Variable temperature NMR experiments have shown that these compounds do react with solvents such as DMSO to afford substituted species, presumably through solvolysis of the halide. Lastly, these compounds are colored due to a MLCT band. We are continuing our work with these complexes to investigate both their physical and chemical properties as well as evaluate them as precursors for bifunctional chelate-based imaging agents.

## 3. Experimental

### 3.1. Spectroscopic methods and materials

All reagents were purchased from Strem, Acros Organics or Sigma–Aldrich and used as received. UV–Vis absorption experiments were carried out on Hitachi 3100 single monochromator and Hitachi U-2800A UV–Vis spectrophotometers. Solution NMR spectroscopy was performed on Varian VXR 300 MHz and Varian 400 MHz NMR instruments. IR spectra were recorded on a Nicolet NEXUS 870 FT-IR Esp and Perkin Elmer Spectrum One FT-IR spectrometers. Elemental analyses were carried out at the School of Chemical Sciences Microanalytical Laboratory at the University of Illinois at Urbana-Champaign or Atlantic Microlab of Norcross, GA 30091. Mass Spectrometric analyses were carried out at Mass Spectrometry and Proteomics Facility at the Ohio State University in Columbus OH.

**Table 2**
Selected bond lengths and angles for **1**–**6**, **9** and **12**.

| Compound | 1 | 2 | 3 | 4 | 5 | 6 | 9 | 12 |
|---|---|---|---|---|---|---|---|---|
| Re–Cl (Å) | 2.513(4) | | 2.493(3) | | 2.5014(14) | | 2.4811(17) | |
| Re–Br (Å) | | 2.6334(12) | | 2.6252(13) | | 2.633(2) | | 2.6405(14) |
| Re–C(Å) | 1.930(9) | 1.954(7) | 1.928(11) | 1.915(10) | 1.933(6) | 1.902(19) | 1.940(8) | 1.913(10) |
| | 1.894(13) | 1.923(7) | 1.903(16) | 1.961(15) | 1.936(6) | 1.875(17) | 1.913(7) | 1.904(9) |
| | | 1.921(8) | | | 1.908(6) | 1.931(19) | 1.922(7) | 1.917 (10) |
| Re—$N_{oxime}$ (Å) | 2.165(6) | 2.144(6) | 2.161(8) | 2.155(7) | 2.140(4) | 2.144(11) | 2.154(6) | 2.163(7) |
| | | 2.161(5) | | | 2.148(4) | 2.130(12) | | |
| Re—$N_{py}$ (Å) | | | | | | | 2.182(6) | 2.189(7) |
| N–Re–N (°) | 72.5(4) | 72.3(2) | 72.0(4) | 72.1(4) | 72.29(15) | 71.3(4) | 74.0(2) | 72.9(3) |

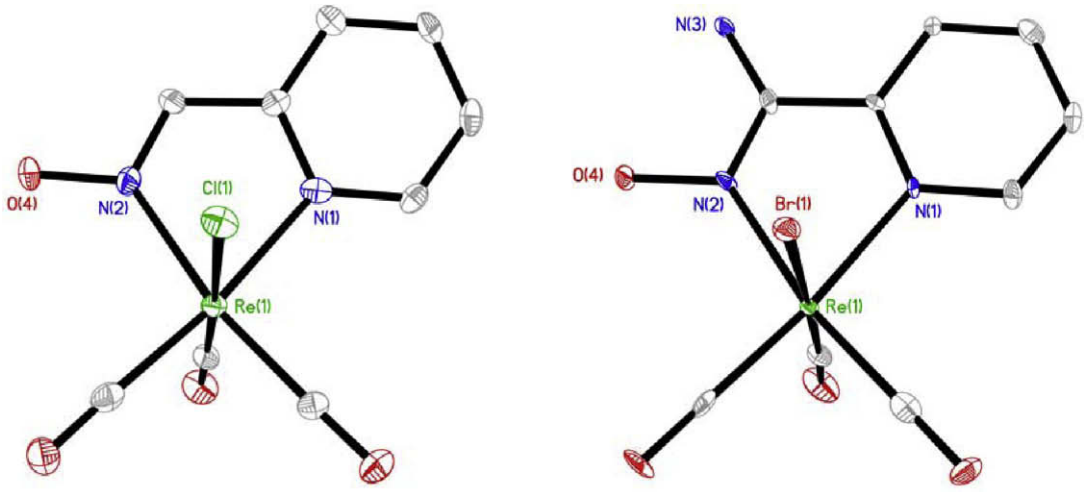


**Fig. 2.** The structures of compounds **9** (left) and **12** (right) with 35% thermal ellipsoids. Hydrogen atoms and solvent have been omitted for clarity.

The synthesis of $[Re(CO)_3(H_2O_3)]Br$ was carried out as previously described [15].

### 3.2. NOESY spectroscopy

Phase sensitive $^1H-{}^1H$ 2D NOESY (Nuclear Overhauser Enhancement Spectroscopy) experiment was carried out at 30 °C on Varian Inova750 MHz spectrometer equipped with the 5mm H/C/N triple resonance Pulsed Field Gradient (PFG) probe. A $^1H$ $\pi/2$ pulse width of 8.6 μs was used in the experiment. The 2D data was collected using a relaxation delay of 2 s and a mixing time of 2 s with the spectral window of 12712.5 Hz in both dimensions. The acquired data consists of 4096 points in F2 dimension and 256 complex points for F1 dimension, with 16 transients for each increment. The data were weighted with shifted sine bell window functions in both dimensions and zero-filled with 4096 × 4096 data points before the final 2D transformation.

### 3.3. X-ray crystallography

X-ray intensity data were measured at 100 K (Bruker KYROFLEX) on a Bruker SMART APEX CCD-based X-ray diffractometer system equipped with a Mo-target X-ray tube ($\lambda$ = 0.71073 Å) operated at 2000 W power. The crystals were mounted on a cryoloop using Paratone N-Exxon oil and placed under a stream of nitrogen at 100 K. The detector was placed at a distance of 5.009 cm from the crystals. The data were corrected for absorption with the SADABS program. The structures were refined using the Bruker SHELXTL Software Package (Version 6.1), and were solved using direct methods until the final anisotropic full-matrix, least squares refinement of $F^2$ converged [16]. Additional experimental detail is provided in Table 1.

*Syntheses of 1, 3 and 5:* The following general procedure was used in each synthesis. $Re(CO)_5Cl$ (150 mg, 0.415 mmol) was mixed with 1 equivalent of ligand (0.415 mmol) and methanol (15 mL) was then added to the flask. During the four hour reflux, the solution turned from colorless to orange-red. Upon completion of the reaction, the solvent was removed by rotary evaporation, resulting in a red, orange or brown solid.

*Synthesis of 2, 4, and 6:* The following general procedure was used in each synthesis. $[Re(CO)_3(H_2O)_3]Br$ (100 mg, 0.247 mmol) was mixed with 1 equivalent of ligand (0.247 mmol). Distilled water (15 mL) was added, and the solution was heated to reflux for 30 min yielding an orange or orange-red solution. Solvent water was removed with a rotary evaporator. Compound **6** was purified with methylene chloride and **2** with acetone then separated via pipette.

*Synthesis of 7 and 8:* The following general procedure was used in each synthesis. $Re(CO)_5Cl$ or $Re(CO)_5Br$ (0.276 mmol) and one equivalent of 1,2-cyclohexanedione dioxime (0.276 mmol) were dissolved in 10 mL of benzene. Reaction mixtures were refluxed for 24 h, and then the solvent was removed by rotary evaporation. Unlike the previous syntheses, these solutions were yellow-brown. The product residues were then purified by column chromatography on silica gel with 15% methanol v/v in ethyl acetate as the eluent. The resultant solution was filtered, and red-black crystals were obtained from slow evaporation.

*Syntheses of 9, 10, 11 and 12:* The following general procedure was used in each synthesis $Re(CO)_5Cl$ or $Re(CO)_5Br$ (0.276 mmol) and one equivalent of either pyridine-2-aldoxime or 2-pyr-

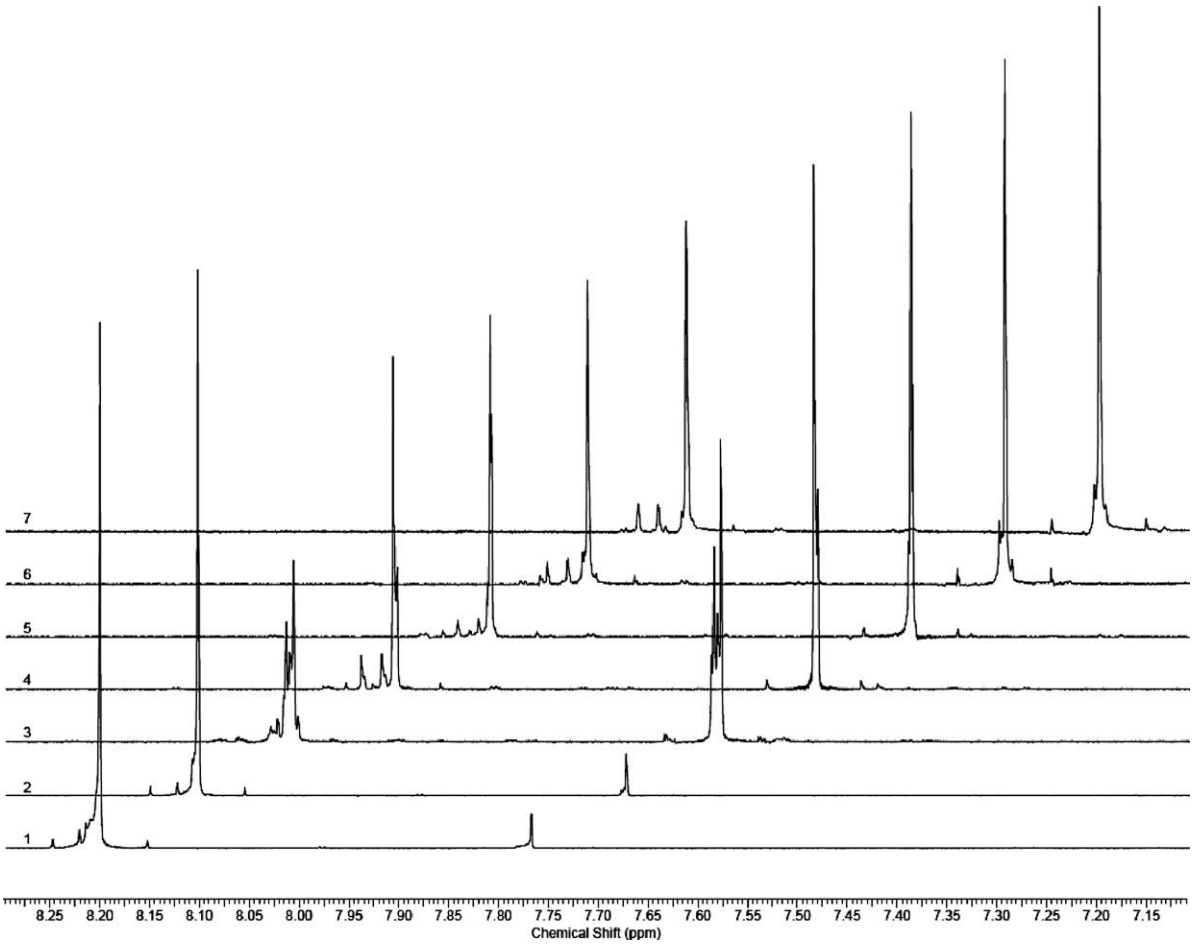


**Fig. 3.** $^{1}$H VTNMR at ten degree increments of the C–H region of **2** in $d^{6}$-DMSO from 40 °C (1) to 100 °C (7).

idylamidoxime (0.276 mmol) were dissolved in either benzene or toluene (10 mL). Reaction mixtures were refluxed for 24 h, and the solvent was removed by rotary evaporation. As the reaction proceeded, the color changed from clear to red. Pure black-red material was isolated upon recrystallization of the reaction residue.

Compound **1**. Yield 132 mg (81%). $^{1}$H NMR (400 MHz, $d_6$-DMSO, $\delta$): 13.31 (s), 11.63 (s), 8.16 (s), 7.73 (s) ppm. $^{13}$C NMR (400 MHz, $d_6$-DMSO) 196.4, 185.8, 150.4, 145.4 ppm. High res. ESI MS (positive ion): 416.9260 (M+Na). CHN Anal. Calc. for $ReC_5H_4O_5N_2Cl$: C, 15.25; H, 1.02; N, 7.11. Found: C, 15.89; H, 1.25; N, 7.17%. IR (CO stretch, cm$^{-1}$): 2036, 1947, 1886. UV–Vis absorption $\lambda_{max}$ (MeOH) 383 nm ($\varepsilon = 3.9 \times 10^3$ M$^{-1}$ cm$^{-1}$). X-ray crystallography: Crystal data and structure refinement parameters are summarized in Table 1.

Compound **2**. Yield 100 mg (92%). $^{1}$H NMR (400 MHz, $d_6$-DMSO, $\delta$): 13.32 (s), 11.65(s) 8.20(s), 7.73(s) ppm. $^{13}$C NMR (400 MHz, $d_6$-DMSO) 195.3, 184.9, 151.3, 147.1 ppm. High res. ESI MS (positive ion): 460.8759 (M+Na). CHN Anal. Calc. for $ReC_5H_4O_5N_2Br$: C, 13.70; H, 0.92; N, 6.39. Found: C 14.79; H, 1.01; N, 6.41%. IR (CO stretch, cm$^{-1}$): 2028, 1876. UV–Vis absorption $\lambda_{max}$ (MeOH) 390 nm ($\varepsilon = 2.9 \times 10^3$ cm$^{-1}$ M$^{-1}$). X-ray crystallography: Crystal data and structure refinement parameters are summarized in Table 1.

Compound **3**. Yield 172 mg (98%). $^{1}$H NMR (400 MHz, $d_6$-acetone, $\delta$): 12.82 (s), 11.65 (s), 2.77 (s), 2.19 (s) ppm.$^{13}$C NMR (400 MHz, $d_6$-acetone): 195.5, 187.1, 161.2, 153.0, 13.7 9.32 ppm. High res. ESI MS (positive ion): 444.9577 (M+Na). CHN Anal. Calc. for $ReC_7H_8O_5N_2Cl$: C, 19.93; H, 1.91; N, 6.64. Found: C, 20.25; H, 1.95; N, 6.70%. IR (CO stretch, cm$^{-1}$): 2032, 1938, 1916. UV–Vis absorption $\lambda_{max}$ (MeOH) 354 nm ($\varepsilon = 3.2 \times 10^3$ cm$^{-1}$ M$^{-1}$). X-ray crystallography: Crystal data and structure refinement parameters are summarized in Table 1.

Compound **4**. Yield 78 mg (67%). $^{1}$H NMR (400 MHz, $d_6$-acetone, $\delta$): 11.73 (s), 2.23 (s) ppm; $^{13}$C NMR (400 MHz, $d_6$-acetone): 195.7, 187.1, 161.8, 153.7, 14.4, 9.90 ppm. High res. ESI MS (positive ion): 488.9072 (M+Na). IR (CO stretch, cm$^{-1}$): 2031, 1938, 1917. CHN Anal. Calc. for $ReC_7H_8O_5N_2Br$: C, 18.03; H, 1.73; N, 6.01. Found: C, 17.98; H, 1.70; N, 5.82%. UV–Vis absorption $\lambda_{max}$ (MeOH) 361 nm ($\varepsilon = 2.8 \times 10^3$ cm$^{-1}$ M$^{-1}$). X-ray crystallography: Crystal data and structure refinement parameters are summarized in Table 1.

Compound **5**. Yield 198 mg (87%). $^{1}$H NMR (300 MHz, $d_6$-DMSO, $\delta$): 7.27 (m), 7.14 (m) ppm; $^{13}$C NMR (400 MHz, $d_6$-DMSO, $\delta$): 196.2, 186.2, 162.0, 130.5, 130.3, 129.6, 128.6 ppm. ESI MS (positive ion): 568.9833 (M+Na) IR (CO stretch, cm$^{-1}$): 2035 (s), 1917 (s). CHN Anal. Calc. for $ReC_{17}H_{12}O_5N_2Cl$: C, 37.39; H, 2.21; N, 5.13. Found: C, 36.96; H, 2.18; N, 5.16%. UV–Vis absorption $\lambda_{max}$ (MeOH) 386 nm ($\varepsilon = 4.3 \times 10^3$ cm$^{-1}$ M$^{-1}$).X-ray crystallography: Crystal data and structure refinement parameters are summarized in Table 1.

Compound **6**. Yield 145 mg (99%). $^{1}$H NMR (300 MHz, $d_6$-DMSO, $\delta$): 12.95 (s), 7.27 (m), 7.12 (m) ppm. $^{13}$C NMR (400 MHz, $d_6$-DMSO, $\delta$): 195.6, 187.1, 162.1, 130.4, 130.3, 129.6, 128.6 ppm. ESI MS (positive ion): 568.9833 (M+Na). IR (CO stretch, cm$^{-1}$): 2036 (s), 1924 (vs) (CO). CHN Anal. Calc. for $ReC_{17}H_{12}O_5N_2Br$: C, 34.58; H, 2.05; N,

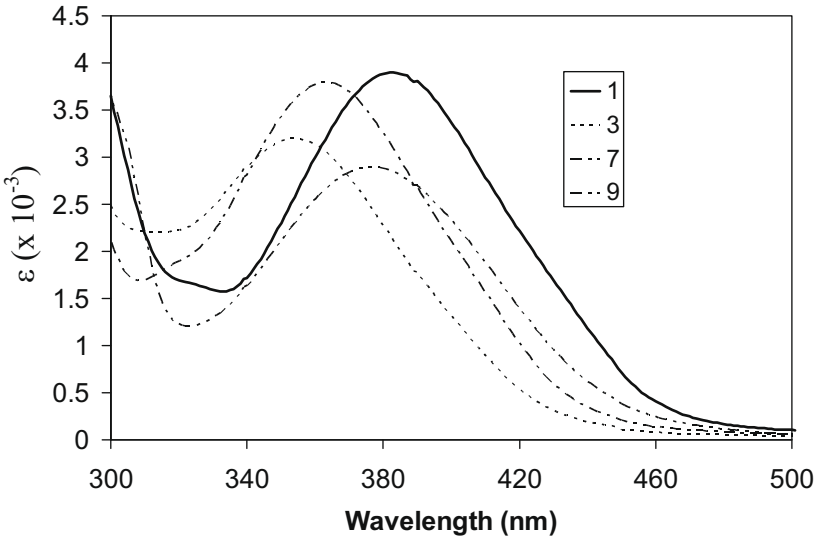


**Fig. 4.** UV-spectra for compounds **1**, **3**,**7** and **9** in methanol.

4.74. Found: C, 34.10; H, 1.96; N, 4.59%. UV–Vis absorption $\lambda_{max}$ (MeOH) 392 nm ($\varepsilon = 4.4 \times 10^3$ cm$^{-1}$ M$^{-1}$). Crystal data and structure refinement parameters are summarized in Table 1.

Compound **7**. Yield 105 mg (85%). $^1$H NMR (300 MHz, $d_6$-DMSO, $\delta$): 12.81(s), 11.62 (s) 2.75 (m), 2.67 (m), 1.63 (m) ppm. $^{13}$C NMR (300 MHz, $d_6$-acetone, $\delta$): 195.4, 187.0, 160.7, 25.9, 19.9 ppm ESI MS (positive ion): 612.9315 (M+Na). IR (CO stretch, cm$^{-1}$): 2029, 1932, 1902. CHN Anal. Calc. for $ReC_9H_{10}O_5N_2Cl$: C, 24.11; H, 2.23; N, 6.25. Found: C, 23.92; H, 1.94; N, 5.93%. UV–Vis absorption $\lambda_{max}$ (MeOH) 364 nm ($\varepsilon = 3.8 \times 10^3$ cm$^{-1}$ M$^{-1}$).

Compound **8**. Yield 103 mg (85%). $^1$H NMR (300 MHz, $d_6$-acetone, $\delta$): 12.62 (s), 2.73 (m), 1.61 (m) ppm. $^{13}$C NMR (300 MHz, $CDCl_3$, $\delta$): 196.5, 185.3, 150.8, 29.8, 16.3 ppm. ESI MS (positive ion): 514.9206 (M+Na). IR (CO stretch, cm$^{-1}$): 2031, 1939, 1922. CHN Anal. Calc. for $ReC_9H_{10}O_5N_2Br$:C, 21.96; H, 2.05; N, 5.69. Found: C, 22.54; H, 2.00; N, 5.47%. UV–Vis absorption $\lambda_{max}$ (MeOH) 369 nm ($\varepsilon = 2.1 \times 10^3$ cm$^{-1}$ M$^{-1}$).

Compound **9**. Yield 108 mg (92%). $^1$H NMR (300 MHz,$d_6$-DMSO, $\delta$): 13.28 (s), 8.94 (d), 8.23 (t), 8.06 (d), 7.66 (t) ppm. $^{13}$C NMR (300 MHz,$d_6$-DMSO, $\delta$): 198.2, 196.3, 188.4, 155.4, 153.5, 153.5, 140.9, 128.4, 127.7 ppm. ESI MS (positive ion): 450.9471 (M+Na); CHN Anal. Calc. for $ReC_9H_6O_4N_2Cl$: C, 25.27; H, 1.41; N, 6.55. Found: C, 25.89; H, 1.23; N, 6.82%. IR (CO stretch, cm$^{-1}$): 2030, 1925, 1878. Crystal data and structure refinement parameters are summarized in Table 1. UV–Vis absorption $\lambda_{max}$ (MeOH) 377 nm ($\varepsilon = 2.9 \times 10^3$ cm$^{-1}$ M$^{-1}$).

Compound **10**. Yield 104 mg (90%). $^1$H NMR (300 MHz, $d_6$-DMSO, $\delta$): 13.29 (s), 8.96 (d), 8.18 (d), 8.09 (t), 8.05 (d) 7.65 (t) ppm. $^{13}$C NMR (300 MHz, $d_6$-DMSO, $\delta$): 197.7, 195.8, 187.7, 173.8, 155.4, 154.1, 153.6, 141.4, 130.2, 128.3 ppm. ESI MS (positive ion): 494.8966(M+Na), CHN Anal. Calc. for $ReC_9H_6O_4N_2Br$: C, 22.89; H, 1.28; N, 5.93. Found: C, 23.77; H, 1.01; N, 5.76%. IR (CO stretch, cm$^{-1}$): 2024, 1934, 1901. UV–Vis absorption $\lambda_{max}$ (MeOH) 386 nm ($\varepsilon = 3.4 \times 10^3$ cm$^{-1}$ M$^{-1}$).

Compound **11**. Yield 104 mg (85%). $^1$H NMR (300 MHz, $d_6$-DMSO, $\delta$): 9.88 (s) 8.00 (d), 7.45 (t), 6.87 ($NH_2$) ppm. $^{13}$C NMR (300 MHz, $d_6$-DMSO, $\delta$): 198.4, 196.9, 189.9, 157.3, 153.3, 149.8, 140.1, 127.8, 123.4 ppm. ESI MS (positive ion): 465.9570(M+Na). CHN Anal. Calc. for $ReC_9H_7O_4N_3Cl$: C, 24.41; H, 1.59; N, 9.49. Found: C, 23.94; H, 1.73; N, 8.98%. IR (CO stretch, cm$^{-1}$): 2021, 1925, 1893. UV–Vis absorption $\lambda_{max}$ (MeOH) 351 nm ($\varepsilon = 4.0 \times 10^3$ cm$^{-1}$ M$^{-1}$).

Compound **12**. Yield 101 mg (85%). $^1$H NMR (300 MHz, $CD_3CN$, $\delta$): 8.90 (s), 8.16 (d), 7.95 (m), 7.62 (m), 6.42 ($NH_2$) ppm; $^{13}$C NMR (300 MHz, $d_6$-DMSO, $\delta$): 198.4, 197.1, 189.9, 157.9, 154.1, 150.5, 140.7, 128.3, 124.0. ESI MS (positive ion): 507.9032 (M+Na). CHN Anal. Calc. for $ReC_9H_7O_4N_3Br$: C, 22.18; H, 1.45; N, 8.62. Found: C, 22.18; H, 1.36; N, 8.25%. IR (CO stretch, cm$^{-1}$): 2022, 1933, 1885. UV–Vis absorption $\lambda_{max}$ (MeOH) 367 nm ($\varepsilon = 4.4 \times 10^3$ cm$^{-1}$ M$^{-1}$). Crystal data and structure refinement parameters are summarized in Table 1.

## Acknowledgements

R.S.H. thanks the Research Corporation (CC6663/6616) for research support and the National Science Foundation for funds to purchase the NMR facilities (CHE-0079348). E.F.P. and J.L. thank the Simeon J. Fortin Charitable trust for summer fellowships. We also wish to acknowledge NSF Grant CHE-0116041 for funds used to purchase the Bruker-Nonius diffractometer.

## Appendix A. Supplementary material

CCDC 712597, 712598, 712599, 712600, 712601, 712602, 712603 and 712604 contains the supplementary crystallographic data for **1**, **2**, **3**, **4**, **5**, **6**, **9** and **12**. These data can be obtained free of charge from The Cambridge Crystallographic Data Centre via www.ccdc.cam.ac.uk/data_request/cif. Supplementary data associated with this article can be found, in the online version, at doi:10.1016/j.jorganchem.2009.02.024.

## References

[1] (a) C. Kaes, A. Katz, M.W. Hosseini, Chem. Rev. 100 (2000) 3553;
(b) D.J. Stufkens, Coord. Chem. Rev. 104 (1990) 39.
[2] (a) F. Hartl, M.P. Aarnts, H.A. Nieuwenhuis, J. van Slageren, Coord. Chem. Rev. 230 (2002) 106;
(b) A. Vlcek, Coord. Chem. Rev. 230 (2002) 225;
(c) J. van Slageren, A. Klein, S. Zalis, D.J. Stufkens, Coord. Chem. Rev. 219 (2001) 937;
(d) A. Vogler, H. Kunkely, Coord. Chem. Rev. 177 (1998) 81.
[3] R.S. Herrick, J. Dupont, I. Wrona, J. Pilloni, M. Beaver, M. Benotti, F. Powers, C.J. Ziegler, J. Organomet. Chem. 692 (2007) 1226.
[4] (a) B.D. Rossenaar, E. Lindsay, D.J. Stufkens Jr., A. Vlcek, Inorg. Chim. Acta 250 (1996) 5;
(b) B.D. Rossenaar, D.J. Stufkens Jr., A. Vlcek, Inorg. Chem. 35 (1996) 2902;
(c) B.D. Rossenaar, C.J. Kleverlaan, M.C.E. van de Ven, D.J. Stufkens, A. Oskam, J. Fraanje, K. Goubitz, J. Organomet. Chem. 493 (1995) 153;

(d) R. Carballo, J.S. Casas, E. Garcia-Martinez, G. Pereiras-Gabian, A. Sanchez, J. Sordo, E.M. Vazquez-Lopez, J.C. Garcia-Monteagudo, U. Abram, J. Organomet. Chem. 656 (2002) 1;
(e) B.D. Rossenaar, D.J. Stufkens Jr., A. Vlcek, Inorg. Chim. Acta 247 (1996) 247;
(f) B.D. Rossenaar, C.J. Kleverlaan, D.J. Stufkens, A. Oskam, J. Chem. Soc., Chem. Commun. (1994) 63;
(g) B.D. Rossenaar, F. Hartl, D.J. Stufkens, Inorg. Chem. 35 (1996) 6194.

[5] (a) L.A. Garcia-Escudero, D. Miguel, J.A. Turiel, J. Organomet. Chem. 691 (2006) 3434;
(b) T. Ederer, R.S. Herrick, W. Beck, Z. Anorg. Allg. Chem. 633 (2007) 235;
(c) R.S. Herrick, T.J. Brunker, C. Maus, K. Crandall, A. Cetin, C.J. Ziegler, Chem. Commun. (2006) 4330;
(d) R.S. Herrick, in: New Developments in Organometallic Research, Nova Science Publishers. Inc., New York, 2006, pp. 115–149;
(e) R.S. Herrick, I. Wrona, N. McMicken, G. Jones, C.J. Ziegler, J. Shaw, J. Organomet. Chem. 689 (2004) 4848;
(f) R.S. Herrick, C.J. Ziegler, H. Bohan, M. Corey, M. Eskander, J. Giguere, N. McMicken, I.E. Wrona, J. Organomet. Chem. 687 (2003) 178;
(g) R.S. Herrick, K.L. Houde, J.S. McDowell, L.P. Kiczek, G. Bonavia, J. Organomet. Chem. 589 (1999) 29;
(h) R. Garcia-Rodriguez, D. Miguel, Dalton Trans. (2006) 1218.

[6] (a) S. Ross, T. Weyhermuller, E. Bill, K. Wieghardt, P. Chaudhuri, Inorg. Chem. 40 (2001) 6656;
(b) D.V. Stynes, I. Vernik, F. Zobi, Coord. Chem. Rev. 233 (2002) 273;
(c) E. Lopez-Torres, U. Abram, Inorg. Chem. 47 (2008) 2890;
(d) I.G. Santos, U. Abram, R. Alberto, E.V. Lopez, A. Sanchez, Inorg. Chem. 43 (2004) 1834;
(e) G. Pereiras-Gabian, E.M. Vazquez-Lopez, H. Braband, U. Abram, Inorg. Chem. 44 (2005) 834;
(f) G. Pereiras-Gabian, E.M. Vazquez-Lopez, U. Abram, Z. Anorg. Allg. Chem. 630 (2004) 1665;
(g) R. Carballo, J.S. Casas, E. Garcia-Martinez, G. Pereiras-Gabian, A. Sanchez, J. Sordo, E.M. Vazquez-Lopez, J.C. Garcia-Monteagudo, U. Abram, J. Organomet. Chem. 656 (2002) 1;
(h) L.S.M. Lam, W.K. Chan, Chem. Phys. Chem. 2 (2001) 252;
(i) N.M. Shavaleev, Z.R. Bell, G. Accorsi, M.D. Ward, Inorg. Chim. Acta 351 (2003) 159;
(j) J. Grewe, A. Hagenbach, B. Stromburg, R. Alberto, E. Vazquez-Lopez, U. Abram, Z. Anorg. Allg. Chem. 629 (2003) 303;
(k) S. Basak, D. Chopra, K.K. Rajak, J. Organomet. Chem. 693 (2008) 2649.

[7] (a) R.S. Herrick, C.J. Ziegler, A. Cetin, T.J. Brunker, Eur. J. Inorg. Chem. 12 (2007) 1632;
(b) B.R. Franklin, R.S. Herrick, C.J. Ziegler, A. Cetin, N. Barone, L.R. Condon, Inorg. Chem. 47 (2008) 5902;
(c) R.S. Herrick, C.J. Ziegler, D.L. Jameson, C. Aquina, A. Çetin, B.R. Franklin, L.R. Condon, N. Barone, J. Lopeza, Dalton Trans. 27 (2008) 2941.

[8] (a) K.E. Linder, M.F. Malley, J.Z. Gougoutas, S.E. Unger, A.D. Nunn, Inorg. Chem. 29 (1990) 2428;
(b) E.N. Treher, L.C. Francesconi, J.Z. Gougoutas, M.F. Malley, A.D. Nunn, Inorg. Chem. 28 (1989) 3411.

[9] (a) K.E. Linder, M.D. Wen, D.P. Nowotnik, M.F. Malley, J.Z. Gougoutas, A.D. Nunn, W.C. Eckelman, Bioconjugate Chem. 2 (1991) 160;
(b) K.E. Linder, M.D. Wen, D.P. Nowotnik, K. Ramalingam, R.M. Sharkey, F. Yost, R.K. Narra, A.D. Nunn, W.C. Eckelman, Bioconjugate Chem. 2 (1991) 407.

[10] (a) R. Alberto, R. Schibli, A. Egli, A.P. Schubiger, U. Abram, T.A. Kaden, J. Am. Chem. Soc. 120 (1998) 7987;
(b) R. Schibli, R. Schwarzbach, R. Alberto, K. Ortner, H. Schmalle, C. Dumas, A. Egli, P.A. Schubiger, Bioconjugate Chem. 13 (2002) 750.

[11] (a) I. Chakraborty, B.K. Panda, J. Gangopadhyay, A. Chakravorty, Inorg. Chem. 44 (2005) 1054;
(b) S. Jurisson, L. Francesconi, K.E. Linder, E. Treher, M.F. Malley, J.Z. Gougoutas, A.D. Nunn, Inorg. Chem. 30 (1991) 1820;
(c) S.M. Harben, P.D. Smith, R.L. Beddoes, D. Collison, C.D. Garner, J. Chem. Soc., Dalton Trans. (1997) 2777;
(d) S. Jurisson, M.M. Halihan, J.D. Lydon, C.L. Barnes, D.P. Nowotnik, A.D. Nunn, Inorg. Chem. 37 (1998) 1922;
(e) L. Cuesta, M.A. Huertos, D. Morales, J. Pérez, L. Riera, V. Riera, D. Miguel, A. Menéndez-Velázquez, S. García-Granda, Inorg. Chem. 46 (2007) 2836.

[12] (a) M. Busby, D.J. Liard, M. Motevalli, H. Toms Jr., A. Vlcek, Inorg. Chem. Acta 357 (2004) 167;
(b) A.J. Graham, D. Akrigg, B. Sheldrick, Cryst. Struct. Commun. 6 (1977) 577;
(c) S.H. Chan, L.S.M. Lam, C.W. Tse, K.Y.K. Man, W.T. Wong, A.B. Djurisic, W.K. Chan, Macromolecules 36 (2003) 5482;
(d) A.M.B. Rodriguez, A. Gabrielsson, M. Motevalli, P. Matousek, M. Towrie, J. Sebera, S. Zalis Jr., A. Vlcek, J. Phys. Chem. A 109 (2005) 5016;
(e) B.D. Rossenaar, C.J. Kleverlaan, M.C.E. van de Ven, D.J. Stufkens, A. Oskam, J. Fraanje, K. Goubitz, J. Organomet. Chem. 493 (1995) 153.

[13] M. Casanova, E. Zangrando, F. Munini, E. Iengo, E. Alessio, Dalton Trans. (2006) 5033.

[14] (a) D.J. Stufkens, Comment Inorg. Chem. 13 (1992) 359;
(b) L.A. Sacksteder, M. Lee, J.N. Demas, B.A. DeGraff, J. Am. Chem. Soc. 115 (1993) 8230.

[15] N. Lazarova, S. James, J. Babich, J. Zubieta, Inorg. Chem. Commun. 7 (2004) 1023.

[16] G.M. Sheldrick, SHELXTL, Crystallographic Software Package, Version 6.10, Bruker-AXS, Madison, WI, 2000.